

# Why the $p$ -norms $p=1$ , $p=2$ and $p=\infty$ are so special? An answer based on spatial uniformity

Carlos Pinzón

November 2024

## Abstract

Among all metrics based on  $p$ -norms, the Manhattan ( $p=1$ ), euclidean ( $p=2$ ) and Chebyshev distances ( $p=\infty$ ) are the most widely used for their interpretability, simplicity and technical convenience. But these are not the only arguments for the ubiquity of these three  $p$ -norms. This article proves that there is a volume-surface correspondence property that is unique to them. More precisely, it is shown that sampling uniformly from the volume of an  $n$ -dimensional  $p$ -ball and projecting to its surface is equivalent to directly sampling uniformly from its surface if and only if  $p$  is 1, 2 or infinity. Sampling algorithms and their implementations in Python are also provided.

## 1 Introduction

The  $p$ -norms are a family of functions that measure the length  $\|\mathbf{x}\|_p$  of  $n$ -dimensional vectors  $\mathbf{x} \in \mathbb{R}^n$  as

$$\|\mathbf{x}\|_p \stackrel{\text{def}}{=} \begin{cases} (\sum_{i=1}^n |x_i|^p)^{1/p} & \text{if } p \in (0, \infty) \\ \lim_{p \rightarrow \infty} \|\mathbf{x}\|_p = \max_{i=1}^n |x_i| & \text{if } p = \infty, \end{cases}$$

and due to the rich structure that these  $p$ -norms induce in the space of vectors, they are encountered very frequently in many areas of mathematics, statistics, and machine learning.

In mathematics, for instance, for  $p \geq 1$ , the  $p$ -distance function  $(\mathbf{x}, \mathbf{y}) \mapsto \|\mathbf{x} - \mathbf{y}\|_p$  is a metric for  $\mathbb{R}^n$ . This metric, called the Minkowski distance, is the basis for more complex and deeply studied metric spaces in mathematics such as

- the space  $\ell^p$  of infinite real sequences  $(x_i)_{i=1}^{\infty}$  whose  $p$ -norm is bounded, where  $\|x\|_p \stackrel{\text{def}}{=} (\sum_{i=1}^{\infty} x_i^p)^{1/p}$  for  $p < \infty$  and  $\|x\|_{\infty} \stackrel{\text{def}}{=} \lim_{p \rightarrow \infty} \|x\|_p = \sup_i x_i$  —the supremum, and
- the space  $L^p$  of functions  $f : \mathbb{R}^n \rightarrow \mathbb{R}$  whose  $p$ -norm is bounded, where

$$\|f\|_p \stackrel{\text{def}}{=} \left(\int_{\mathbb{R}^n} |f(x)|^p dx\right)^{1/p} \text{ for } p < \infty \text{ and } \|f\|_\infty \stackrel{\text{def}}{=} \lim_{p \rightarrow \infty} \|f\|_p = \text{ess sup}_x |f(x)| \text{ —the essential supremum}^1.$$

In machine learning, the  $p$ -norms are used as regularization penalties to reduce overfitting —mainly L1 and L2 penalties, and as loss functions in regression problems. In statistics, the  $p$ -norms can be used to define the most fundamental central tendency statistics as  $m_p(X) \stackrel{\text{def}}{=} \inf_m E(\|X - m\|_p)$ . Notably, the mean occurs with  $p = 2$ , the median with  $p = 1$ , the midrange with  $p = \infty$ , and as some authors suggest, the mode with “ $p = 0$ ”, an abuse of notation that is arguably wrong because three different limits occur as  $p \rightarrow 0^+$ . Namely, one obtains the geometric mean via  $\|x\|_p (1/n)^{1/p} \rightarrow (\prod_{i=1}^n x_i)^{1/n}$ , the counting measure via  $\|x\|_p^p \rightarrow \sum_{i=1}^n \mathbf{1}\{x_i \neq 0\}$  (this is the one related to the mode), and the plain limit  $\|x\|_p \rightarrow \infty$  for all  $x \neq 0$ .

Geometrically, the  $p$ -norms have a clear interpretation for  $p \in \{1, 2, \infty\}$ . By considering all points in  $\mathbb{R}^n$  at  $p$ -distance at most 1 and exactly 1 from a given central point, we obtain the  $p$ -ball and the  $p$ -sphere respectively, and these have simple geometrical shapes for  $p \in \{1, 2, \infty\}$ , e.g. a rhomb, a circle and a square for  $n = 2$ . For these values of  $p$ , the Minkowski distance receives special names. It is called Manhattan or taxicab distance for  $p = 1$ , euclidean distance for  $p = 2$  and Chebyshev or maximum distance for  $p = \infty$ . For other values of  $p$  the  $p$ -norms are less studied, perhaps because of unrealistic or unclear semantics and mere algebraic inconvenience.

In this paper, we show that the values  $p \in \{1, 2, \infty\}$  are not merely more practical in terms of geometry or algebra, but they are also special in terms of spatial uniformity. We prove that these norms and only these norms have the property that the  $n$ -dimensional volumetrically uniform distribution on the  $p$ -ball induces the  $(n - 1)$ -dimensional superficially uniform distribution on the  $p$ -sphere via a linear projection.

## 2 Squigonometric functions

In order to parametrize the  $p$ -sphere and the  $p$ -ball in 2 dimensions, called  $p$ -circle in that case, this paper uses the so-called *squigonometric functions* [24]<sup>2</sup>. The parametrization of the circumference (visible in Figure 2) is analogous to  $(\cos(t), \sin(t))$  varying  $t$  in  $[0, 2\pi]$ , except that  $\pi$  and the functions sine and cosine become  $\pi_p$ ,  $\cos_p(t)$  and  $\sin_p(t)$  (depicted in Figure 1), with the following properties:

1.  $\pi_p$  is the area of the  $p$ -circle.
2.  $\|(\cos_p(t), \sin_p(t))\|_p = 1$  for all  $t \in \mathbb{R}$ .

<sup>1</sup>Defined as the infimum of all real numbers that upper bound  $f$  almost everywhere.

<sup>2</sup>Curiosity. The prefix “squi-” comes from the resemblance of a  $p$ -circle, or “squirecle”, between a square ( $p = \infty$ ) and a circle ( $p = 2$ ).

3.  $\cos_p(t) = \cos_p(-t) = \sin_p(t - \pi_p/2)$  for all  $t \in \mathbb{R}$ .

More precisely, from Section 3.1 of [24],  $\sin_p(t)$  and  $\cos_p(t)$  are defined for  $p < \infty$  as the unique solution to the coupled initial value problem

$$C'(t) = -S(t)^{p-1}; \quad S'(t) = C(t)^{p-1}; \quad C(0) = 1; \quad S(0) = 0, \quad (1)$$

which converge as  $p \rightarrow \infty$ , to  $\sin_\infty(t) \stackrel{\text{def}}{=} \cos_\infty(t - 2)$  and

$$\cos_\infty(t) \stackrel{\text{def}}{=} \begin{cases} \min(1, \max(-1, |t - 4| - 2)) & \text{if } t \in [0, 8] \\ \cos_\infty(t \bmod 8) & \text{otherwise.} \end{cases}$$

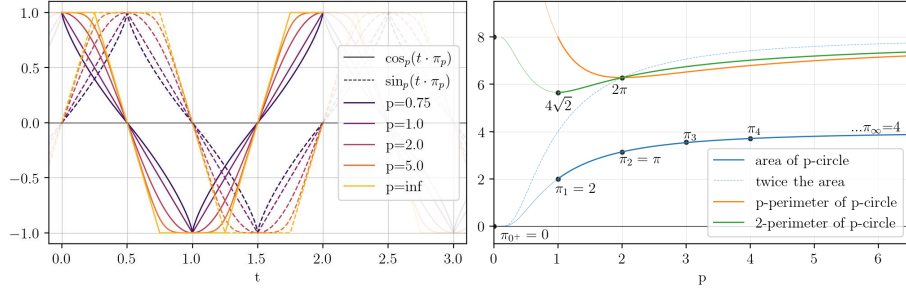


Figure 1: Squigonometric functions (left) and areas and perimeters of the unit  $p$ -circle in different  $p$ -norms (right).

### 3 Area-length correspondence in 2D

Let us concentrate on the first quadrant of the  $p$ -circle, parametrized as the set  $\{(\cos_p(t), \sin_p(t)) : t \in [0, \pi_p/2]\}$ . In reference to Figure 2, define  $A(t)$  as the area of the orange shade, which is enclosed by the circumference of the  $p$ -circle to the right, by the x-axis to the bottom, and by the line that crosses  $(0, 0)$  and  $(\cos_p(t), \sin_p(t))$  to the top, and let  $\ell_{p,q}(t)$  be the  $q$ -length of the black curve  $(1, 0)$  to  $(\cos_p(t), \sin_p(t))$ . The parameter  $q$  defines how the length is measured, e.g.  $q = 2$  for the euclidean length,  $q = 1$  for the Manhattan length, and  $q = \infty$  for the Chebyshev length. The only relevant values for  $q$  are  $q = p$  (the metric induced by  $p$ ) and  $q = 2$  for reference.

The  $q$ -length, can be computed as  $\ell_{p,q}(t_0) = \int_0^{t_0} d\ell_{p,q}(t)$ , where the infinitesimal  $d\ell_{p,q}(t)$  is the  $q$ -norm of a triangle with sides  $d\cos_p(t)$  and  $d\sin_p(t)$ . Following the ODE in Equation (1) for  $p < \infty$ , the two sides become  $-\sin_p(t)^{p-1} dt$  and  $\cos_p(t)^{p-1} dt$  respectively, and for  $p = \infty$ , the triangle degenerates into a single line of length  $dt$  (regardless of  $q$ ). Hence,

$$\frac{d\ell_{p,q}(t)}{dt} = \begin{cases} \|(\cos_p(t)^{p-1}, \sin_p(t)^{p-1})\|_q & \text{if } p < \infty \\ 1 & \text{if } p = \infty. \end{cases} \quad (2)$$

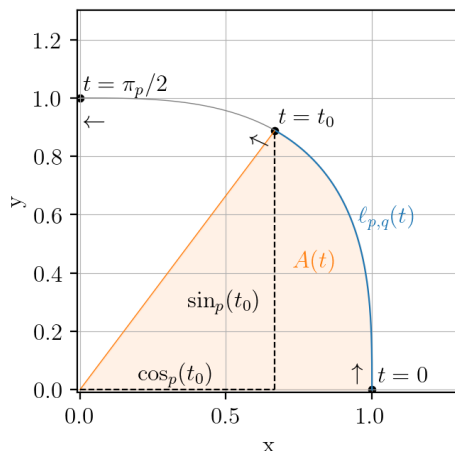


Figure 2: 2D parametrization

It is known that  $A(t)$  is proportional to  $t$  (more precisely  $A(t) = \frac{t}{2}$ ), which is why this parametrization is called area-based [24], pages 59-60. Indeed, since

$$\begin{aligned}
 A(t_0) &= \int_{\pi_p/2}^{t_0} \cos_p(t) \frac{\sin_p(t_0)}{\cos_p(t_0)} d \cos_p(t) + \int_{t_0}^0 \sin_p(t) d \cos_p(t) \\
 &= \frac{\sin_p(t_0)}{\cos_p(t_0)} \frac{\cos_p(t)^2}{2} \Big|_{\pi_p/2}^{t_0} + \int_{t_0}^0 \sin_p(t) d \cos_p(t) \\
 &= \frac{1}{2} \sin_p(t_0) \cos_p(t_0) + \int_{t_0}^0 \sin_p(t) d \cos_p(t), \tag{3}
 \end{aligned}$$

then,

$$\frac{dA(t)}{dt} = \frac{1}{2} \cos_p(t)^p - \frac{1}{2} \sin_p(t)^p - \sin_p(t)^p = \frac{1}{2} (\cos_p(t)^p + \sin_p(t)^p) = \frac{1}{2}. \tag{4}$$

With equations (2) and (4), we can prove the following proportionality relationship between  $A(t)$  and  $\ell_{p,q}(t)$ .

**Proposition 1.** *The functions  $A(t)/A(\pi_p/2)$  and  $\ell_{p,p}(t)/\ell_{p,p}(\pi_p/2)$  of relative area and relative  $p$ -length for  $t \in [0, \pi_p/2]$  are equal if and only if  $p \in \{1, 2, \infty\}$ . Moreover, these functions are also equal to  $\ell_{p,2}(t)/\ell_{p,2}(\pi/2)$  if and only if  $p \in \{1, 2, \infty\}$ .*

*Proof.* Let  $q > 0$  be the norm used for measuring the relative length. Since the relative functions are already equal at 0 and 1, taking values 0 and 1 respectively, it suffices to show that  $A'(t) \propto \ell_{p,q}'(t)$ . From Equation (4), we have  $A'(t) = 1/2$ , so the problem reduces to show that  $\ell_{p,q}'(t)$  is a positive constant. From Equation (2), it's clear that there are only three cases in which  $\ell_{p,q}'(t)$  is constant:

1.  $p = \infty$  forces  $\ell_{p,q}'(t) = 1$  explicitly for all  $q$ ;
2.  $p = 1$  forces  $\ell_{p,q}'(t) = \|(1, 1)\|_q$  which is constant for all  $q$ ;
3. if  $(p - 1)q = p$ , then the property  $\cos_p(t)^p + \sin_p(t)^p = 1$  can be used in Equation (2) to obtain  $\ell_{p,q}'(t) = (\cos_p(t)^{(p-1)q} + \sin_p(t)^{(p-1)q})^{1/q} = 1$ , and this only happens when  $p = \frac{q}{q-1}$ .

With the additional constraint that  $q \in \{2, p\}$ , there are only five solutions, which are  $(p, q) \in \{(1, 1), (1, 2), (2, 2), (\infty, 2), (\infty, \infty)\}$ .  $\square$

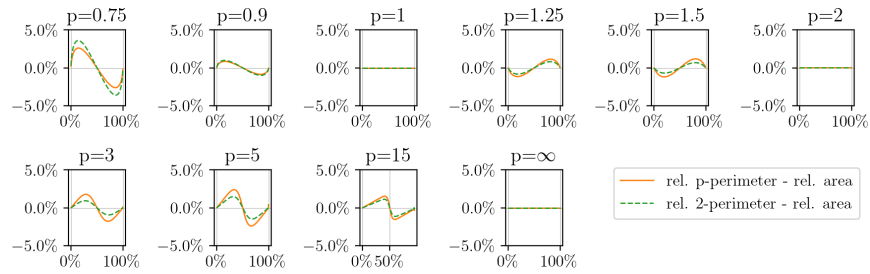


Figure 3: Difference between relative perimeters (cumulative divided by total) and relative area varying  $t \in [0, \pi_p/2]$ . The x-axis is the relative area. The two curves are zero only for  $p \in \{1, 2, \infty\}$ .

As a consequence of Proposition 1, it is not the same to sample uniformly from (the area of) the  $p$ -circle and project to its circumference, as it is to sample uniformly from its circumference directly, unless and only unless  $p \in \{1, 2, \infty\}$ . This is shown in Figure 3.

### 3.1 If there is a $p$ -length, why not a $p$ -area?

Notice that the sides of a rectangle with vertices  $(0, 0)$ ,  $(a, 0)$ ,  $(0, b)$ ,  $(a, b)$  are  $a$  and  $b$  regardless of the  $p$ -norm being used, hence the area is independent of  $p$ , at least for straight (non-tilted) rectangles. If we assume the following minimal assumptions for a notion of area,

1. the area of any figure is non-negative,
2. the area of the union of disjoint pieces gives the sum of their areas, and
3. translation invariance,

then, it follows that the area of any (non-fractal or pathologic) 2D figure can be approximated with the sum of areas of many tiny disjoint rectangles that cover it. For non-pathologic figures, the total area of the rectangles that touch the figure border (overestimating the total area) converges to zero as the resolution increases, hence also the error of the approximation converges to zero. Since this limiting procedure yields the same result independently of the norm  $p$  used

to measure the sides of the rectangles, the notion of area for figures in  $\mathbb{R}^2$  is independent of  $p$  and coincides with the classic euclidean measure of area.

For length, however, when segmenting a curve into infinitesimal diagonal segments, the length of each diagonal depends on the spatial norm. While it could be argued that if the curve was segmented into horizontal and vertical segments, the length would be the same for all  $p$ -norms, this is known to be an invalid approximation for the length of a curve.

For surfaces in 3D, the approximation consists of infinitesimal inclined planes, and the area of each plane depends on the  $p$ -norm used to measure its diagonal sides. The same dependency holds for lengths in 3D, while the volume in 3D is the same for all  $p$ -norms as it is approximated with straight cubes. More generally, for  $\mathbb{R}^n$  endowed with the  $p$ -norm, the  $n$ -dimensional measure does not depend on  $p$  but all  $k$ -dimensional measures with  $1 \leq k < n$  do.

An important remark is that the lengths of the diagonals and the area of inclined planes must be computed without rotating them, because all  $p$ -norms are sensitive to rotations, except only for the euclidean norm. More precisely, as shown in Theorem 5.5 of [16], when  $p \in [1, \infty)$  but  $p \neq 2$ , there are only 8 isometries (transformations that preserve size) in 2D that fix the origin (to exclude translations), namely, the identity, the reflections across the  $y$ -axis,  $x$ -axis, the line  $y = x$ , the line  $y = -x$ , and the rotations by  $\pi/2$ ,  $\pi$ , and  $-\pi/2$ . So there are only 4 rotations for  $p \neq 2$  (defining a rotation in 2D as an isometry that fixes the origin and only the origin), while for  $p = 2$  there are infinitely many. For this reason, at least from an abstract point of view,  $p = 2$  provides the richest structure and is the most special of all  $p$ -norms.

## 4 Volume-surface correspondence in nD

Consider the surface  $\text{Sph}_p^n$  of the  $n$ -dimensional  $p$ -ball. As in the 2D case, we will focus on the subset in which all coordinates are non-negative. Let us call this set the *unsigned  $n$ -dimensional  $p$ -sphere*, denoted  $|\text{Sph}_p^n|$ , with absolute value in the notation to denote non-negativity. Figure 4 shows an instance of  $|\text{Sph}_p^n|$ .

To parametrize the unsigned  $p$ -sphere, let us use the following recurrence formula that simplifies the generalization to  $n$  dimensions. Let the last coordinate be given by  $z \stackrel{\text{def}}{=} \cos_p(t)$  and the remaining by  $\sin_p(t)x_i$  for  $t \in [0, \pi_p/2]$  and  $(x_1, \dots, x_{n-1}) \in |\text{Ball}_p^{n-1}|$ .

The objective is to compare the hyper-volume  $V(t)$  enclosed by the light blue and green shades, with the *hyper-area*<sup>3</sup>  $S_q(t)$  of the light blue shade. For this comparison, we shall introduce two constants. Let  $R$  be the hyper-area of the orange shade, which is contained in the hyper-plane  $z = 0$ , and let  $P_q$  be the *hyper-length*<sup>4</sup> of its solid orange border.

<sup>3</sup>This means area in 3D, volume in 4D,  $(n - 1)$ -dim.-volumes in  $n$ D, and length in 2D.

<sup>4</sup>This means length in 3D, area in 4D, volume in 5D, etc., and set cardinality in 2D.

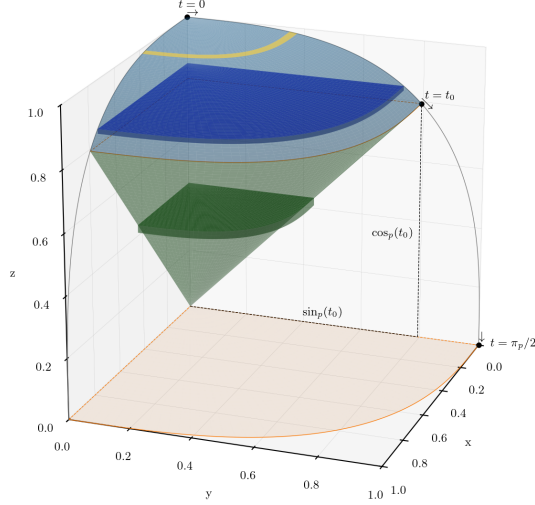


Figure 4: Parametrization of an unsigned  $(n=3)$ -dimensional  $(p=4)$ -ball showing differential volume disks (dark blue, dark green) and surface slices (yellow).

The hyper-area  $R$  does not depend on  $Q$ , because it is the mass of an  $n - 1$ -dimensional object that is embedded in  $n - 1$  dimensions without rotation (by discarding the last dimension). However, the hyper-length  $P_q$  does depend on  $q$ , analogously to the discussion in the previous section. In particular, for  $n = 3$ ,  $P_q$  coincides with  $\ell_{p,q}(\pi_p/2)$  and  $R$  with  $A(\pi_p/2)$ .

To integrate the volume, we shall consider the dark blue and dark green hyper-disks of differential heights. The top and bottom hyper-surfaces of these hyper-disks, are scaled versions of the same orange shape. Notice that when this shape is scaled on every dimension by a factor  $c$ , the hyper-area changes by a factor  $c^{n-1}$ , because  $p$ -norms are linear to scalar multiplication and the shape is  $(n - 1)$ -dimensional. Hence, the hyper-area of the blue hyper-disk contained in the plane  $z = \cos_p(t)$  for some  $t$  is  $\sin_p(t)^{n-1}R$ , and the hyper-area of the dark green hyper-disk at height  $z = \cos_p(t)$ , is  $R \cos_p(t) \left( \frac{\sin_p(t_0)}{\cos_p(t_0)} \right)^{n-1}$ . This yields

$$\begin{aligned}
V(t_0) &= \int_0^{t_0} R \sin_p(t)^{n-1} d \cos_p(t) + \int_{t_0}^{\pi_p/2} R \left( \frac{\sin_p(t_0) \cos_p(t)}{z(t_0)} \right)^{n-1} d \cos_p(t) \\
&= R \int_0^{t_0} \sin_p(t)^{n-1} d \cos_p(t) + R \frac{\sin_p(t_0)^{n-1}}{z(t_0)^{n-1}} \frac{\cos_p(t)^n}{n} \Big|_{t_0}^{\pi_p/2} \\
&= R \int_0^{t_0} \sin_p(t)^{n-1} d \cos_p(t) + \frac{R}{n} \sin_p(t_0)^{n-1} z(t_0)
\end{aligned}$$

from which we can conclude that  $V(t)$  is differentiable and its derivative is

$$\begin{aligned}
\frac{dV(t)}{dt} &= R \sin_p(t)^{n-1} \frac{d \cos_p(t)}{dt} - \frac{R}{n} \frac{d}{dt} (\sin_p(t)^{n-1} \cos_p(t)) \\
&= R \sin_p(t)^{n+p-2} + \frac{R(n-1)}{n} \sin_p(t)^{n-2} \cos_p(t)^p - \frac{R}{n} \sin_p(t)^{n+p-2} \\
&= \frac{R}{n} \sin_p(t)^{n-2} (n \sin_p(t)^p + (n-1) \cos_p(t)^p - \sin_p(t)^p) \\
&= \frac{R}{n} \sin_p(t)^{n-2} (n-1).
\end{aligned}$$

Therefore, the hyper-volume can be expressed more succinctly as

$$V(t_0) = \frac{R \cdot (n-1)}{n} \int_0^{t_0} \sin_p(t)^{n-2} dt \quad (5)$$

To integrate the hyper-surface, consider the differential surface slice in yellow, which forms an annulus, i.e. the shape of a flat washer. The width of the annulus is  $d\ell_{p,q}(t)$  (a differential length along the gray curve), while the hyper-length can be computed by scaling  $P_q$  by a factor of  $\sin_p(t)$ , i.e.  $\sin_p(t)^{n-2}$  to account for all dimensions. The hyper-area of the annulus is therefore  $P_q \sin_p(t)^{n-2} d\ell_{p,q}(t)$ , and that of the hyper-surface is

$$S_q(t_0) = P_q \int_0^{t_0} \sin_p(t)^{n-2} d\ell_{p,q}(t) \quad (6)$$

Putting together Equations (5) and (6), we can prove the following proposition that generalizes Proposition 1.

**Proposition 2.** *For all  $n \geq 2$ , the functions  $V(t)/V(\pi_p/2)$  and  $S_p(t)/S_p(\pi_p/2)$  of relative hyper-volume and relative hyper- $p$ -area for  $t \in [0, \pi_p/2]$  are equal if and only if  $p \in \{1, 2, \infty\}$ . Moreover, these functions equal also  $S_2(t)/S_2(\pi/2)$  if and only if  $p \in \{1, 2, \infty\}$ .*

*Proof.* As in the 2-dimensional case (Proposition 1), the relative functions are already equal at 0 and 1, so the problem is equivalent to showing that  $V'(t) \propto S_p'(t)$ , which according to formulas (5) and (6) is equivalent to showing that  $\ell_{p,q}'(t)$  is constant. From the proof of Proposition 1, it follows that this occurs with  $q \in \{p, 2\}$  if and only if  $p \in \{1, 2, \infty\}$ .  $\square$

As a consequence of Proposition 2, it can be concluded for all  $n$  that it is not the same to sample uniformly from the hyper-volume of a  $p$ -ball and project to its hyper-surface, as it is to sample uniformly from its hyper-surface directly, unless and only unless  $p \in \{1, 2, \infty\}$ .

The proof of Proposition 2 does not require to determine the constants  $R$  and  $P_q$  in Equations (5) and (6). For completeness, we show how to compute these



next. Let  $V_n \stackrel{\text{def}}{=} 2^n V(\pi_p/2)$  denote the total volume of the  $n$ -dimensional  $p$ -ball, and  $S_{n,q} \stackrel{\text{def}}{=} 2^n S_q(\pi_p/2)$  its total hyper-area. Under this notation, we have  $R = V_{n-1}/2^{n-1}$  and  $P_q = S_{n-1,q}/2^{n-1}$ . Using Equations (5) and (6), we obtain recursive formulas for  $V_n$  and  $S_{n,q}$ , whose simplification leads to

$$V_n = 2^{n-1} \prod_{k=0}^{n-2} \int_0^{\pi_p/2} \sin_p(t)^k dt,$$

$$S_{n,q} = \frac{2^{n-1}}{n} \prod_{k=0}^{n-2} \int_0^{\pi_p/2} \sin_p(t)^k d\ell_{p,q}(t).$$

## 5 Sampling uniformly in the $p$ -ball

In this section we develop and discuss computational methods to sample uniformly from the unitary  $p$ -ball in  $n$  dimensions, both volumetrically inside the ball and superficially on the frontier. An implementation of these algorithms in Python can be found in the appendix.

### 5.1 Algorithms based on squigonometry

Based on the results of the previous section, particularly on the recursive construction of the unsigned  $p$ -sphere as well as Equations (5) and (6), we can derive the following algorithms by sampling coordinate by coordinate recursively.

**Algorithms V1 and S1.** Generators of random samples from the  $n$ -dimensional unitary  $p$ -ball. Samples from Algorithm **V1** are uniformly distributed in the hyper-volume (in any  $q$ -norm). Samples from Algorithm **S1** are uniformly distributed on the hyper-surface in the specified  $q$ -norm.

1. Let  $X_1 = 1$ .
2. For  $k = 2..n$ :
  - (a) Sample  $T_k \in [0, \pi_p/2]$  with law  $f_{T_k}(t)$ , defined as:

For Algorithm <b>V1</b> (volume),	$f_{T_k}(t) \propto \sin_p(t)^{k-2}$ .
For Algorithm <b>S1</b> (surface),	$f_{T_k}(t) \propto \sin_p(t)^{k-2} \frac{d\ell_{p,q}(t)}{dt}$ .
  - (b) Let  $X_k = \cos_p(T_k)$ .
  - (c) Update  $X_i \leftarrow \sin_p(T_k) X_i$  for all  $i = 1, 2, \dots, k-1$ .
3. Sample signs  $S_1, \dots, S_n \sim \text{Uni}\{-1, 1\}$ .
4. Return  $(S_i X_i)_{i=1}^n$ .

The implementation of these algorithms has the challenges of computing  $\cos_p(t)$  and  $\sin_p(t)$ , and above all, sampling  $T_k$  from  $f_{T_k}(t)$ . By using a fine grid over a

single unsigned  $p$ -sphere in 2 dimensions, it is possible to accurately approximate the inverse  $p$ -cosine and  $p$ -sine functions as well as the cumulative distribution function (CDF) of  $f_{T_k}(t)$  for each value of  $k$ . These functions can then be inverted using interpolation to obtain  $\cos_p(t)$  and  $\sin_p(t)$  and to sample  $T_k$ . For a complete implementation, refer to the code in the appendix.

## 5.2 The $p$ -normal distributions

The gaussian distribution has the distinctive property that if  $X$  and  $Y$  are independent and gaussian, then the joint density function  $f_{X,Y}(x,y)$  of the vector  $(X,Y)$  is isotropic (i.e. radially symmetric), as it can be written as a function of the euclidean norm  $f_{X,Y}(x,y) = f(x)f(y) = g(\|(x,y)\|_2)$ . Moreover, the joint of independent distributions is isotropic if and only if it is a scaled version of the gaussian.

The argument is the following<sup>5</sup>. For  $y = 0$  we have  $f(x)f(0) = g(|x|)$ , so letting  $a = \sqrt{|x|}$ ,  $b = \sqrt{|y|}$ , and  $h(r) \stackrel{\text{def}}{=} g(\sqrt{r})/f(0)^2$ , the radial symmetry equation becomes

$$h(a^2)h(b^2) = \frac{g(a)}{f(0)^2} \frac{g(b)}{f(0)^2} = \frac{f(\pm a)}{f(0)} \frac{f(\pm b)}{f(0)} = \frac{g(\|(\pm a, \pm b)\|_2)}{f(0)^2} = h(a^2 + b^2).$$

This functional equation is known as the Exponential Cauchy's Functional Equation [12], and the only non-degenerate<sup>6</sup> solution is known to be the exponential function [8, 23]  $h(a) = e^{c \cdot a}$ . Therefore,  $f$  must be given by  $f(x) = f(0) e^{-c|x|^2}$  for some constant  $c$ . For  $f$  to be a density, we must have  $c > 0$  and  $f(0) = c/\sqrt{2\pi}$ , where the mysterious appearance of the constant  $\pi$  is due precisely to the radial symmetry of the gaussian, a beautiful connection and celebrated fact for which at least 11 different proofs have been found [6].

With a similar argument, it can be shown that a distribution is radially symmetric in the  $p$ -norm for  $p < \infty$  if and only if it is given by  $f(x) = f(0) e^{-c|x|^p}$  for some constant  $c > 0$ . For  $p = \infty$ , the argument is slightly different. If  $f(y) > 0$  for some  $y > 0$ , then for all  $x \in [0, y]$ , we have  $f(\pm x)f(\pm y) = g(\|(x,y)\|_\infty) = g(y)$ , so  $f$  is constant on  $[-y, y]$ . Therefore,  $f$  must be given by  $f(x) = f(0)\mathbf{1}\{|x| < c\}$  for some  $c > 0$ .

Both for  $p < \infty$  and  $p = \infty$ , the scale of  $f$  can be chosen arbitrarily in principle, but for the purposes of this paper, we define the  $p$ -normal distribution  $f_p$  as

$$f_p(x) \stackrel{\text{def}}{=} c_p \exp(-|x|^p/p) \quad ; \quad c_p = \frac{1}{2^{\frac{1}{p}} \Gamma(1 + 1/p)},$$

$$f_\infty(x) \stackrel{\text{def}}{=} \lim_{p \rightarrow \infty} f_p(x) = c_\infty \mathbf{1}\{|x| < 1\} \quad ; \quad c_\infty = \lim_{p \rightarrow \infty} c_p = \frac{1}{2}, \quad (7)$$

<sup>5</sup>A video visualizing and explaining the proof can be found in [20].

<sup>6</sup>Pathological solutions exist [17] by means of Hamel bases. See [5] for a quick and clear explanation for the "monstrous" solutions to Cauchy's additive functional equation, which are analogous to the exponential via a logarithmic transformation.

where the default scale guarantees that  $E_{X \sim f_p}(\|X\|_p) = 1$ . For different scales ( $b \neq 1$ ), the distribution of  $Y = bX$  is given by  $f_{p,b}(y) = bf_p(y/b)$ .

This distribution has already been investigated with different names in the literature, including the  $\theta$ -normal distribution [9] ( $\propto \exp(-|x|^p)$ ), the General Gaussian distribution [14, 15], and without a particular name in [21]. Except for the lattermost scale factor (as a function of  $p$ ) is different. The reason for this is that these studies are less focused on geometry and more focused on the statistics of the distribution, e.g. the so-called  $L^p$ -variance. In this regard, our paper can be regarded as a bridge between these works that focus in statistics and that of [24], mostly focused on geometry and calculus.

Moreover, Equation (7) also corresponds to a signed power gamma distribution, a particular case of the signed generalized gamma distribution. The generalized gamma has been discussed at least since 1924 [1] with the purpose of studying income curves, and studied in depth since then with different parametrizations and names [22, 11, 13, 18], e.g. generalized Weibull.

Let  $X_1, \dots, X_n$  be i.i.d. random variables with law  $f_p$ . From Equation (7), the law of the vector  $X = (X_1, \dots, X_n)$  is given by

$$\begin{aligned} f_p^{(n)}(x) &\stackrel{\text{def}}{=} f_p(x_1) \cdots f_p(x_n) = \begin{cases} c_p^n \exp(-\|x\|_p^p/p) & \text{if } p < \infty, \\ c_\infty^n \mathbf{1}\{\|x\|_\infty < 1\} & \text{if } p = \infty, \end{cases} \\ &= c_p^{n-1} f_p(\|x\|_p). \end{aligned} \quad (8)$$

with  $c_p$  as indicated in Equation (7). In both cases, the joint density  $f_p^{(n)}$  is  $p$ -isotropic, i.e. radially symmetric in the  $p$ -norm, as it can be written as a function of the the  $p$ -radius  $R_{n,p} = \|X\|_p$ .

The density of  $R_{n,p}$  is given by the integration of Equation (8) over  $p$ -spheres. A  $p$ -sphere of radius  $r$  has a mass proportional to  $r^{n-1}$ , and the density of  $R_{n,p}$  is therefore given by

$$f_{R_{n,p}}(r) \propto r^{n-1} \exp(-(n/p)r^p) \quad ; \quad f_{R_{n,\infty}}(r) \propto r^{n-1} \mathbf{1}\{r < 1\}. \quad (9)$$

By considering a scaled radius  $R_{n,p}^* \stackrel{\text{def}}{=} R_{n,p}/\sqrt[p]{n}$  and with the notation  $\sqrt[p]{n} \stackrel{\text{def}}{=} \lim_{p \rightarrow \infty} \sqrt[p]{n} = 1$ , Equation (7) simplifies Equation (9) into  $f_{R_{n,p}^*}(r) \propto r^{n-1} f_p(r)$ .

### 5.3 Algorithms based on the $p$ -normal distributions

Let  $X$  be the random vector  $X = (X_1, \dots, X_n)$  composed of i.i.d. random coordinates with law  $f_p$ . Since  $X$  is  $p$ -isotropic, for any fixed radius  $r$  and as  $\Delta r \rightarrow 0$ , the conditional distribution of  $X$  given  $\|X\|_p \in (r, r + \Delta r)$  converges to a uniform distribution in its domain—the volume between two  $p$ -spheres with radius difference of  $\Delta r$ .

The conditional distribution of the vector  $\bar{X} \stackrel{\text{def}}{=} X/r$  given  $\|X\|_p \in (r, r + \Delta r)$  also converges as  $\Delta r \rightarrow 0$  to a uniform distribution in the volume between the

$p$ -spheres of radius  $1$  and  $1 + \frac{\Delta r}{r}$ . Notice that the same conclusion is valid for any  $X$  that is  $p$ -isotropic, therefore the distribution of  $\bar{X}$  is invariant.

In particular, if  $V$  is a random vector uniformly distributed in the unitary  $p$ -ball, it is  $p$ -isotropic, hence  $V/\|V\|_p$  is distributed like  $X$ . Furthermore, the distribution of  $R \stackrel{\text{def}}{=} \|V\|_p$  can be obtained from the same observation that produced Equation (9), namely,  $f_R(r) \propto r^{n-1}$ , i.e., a standard power distribution  $R \sim \text{Beta}(1, n)$ , or  $R = U^{1/n}$  where  $U \sim \text{Uni}[0, 1]$ . These two facts can be combined to reconstruct the variable  $V$  as the product  $R\bar{X}$ , as presented in Algorithm V2. However, the same argument does not hold for the hyper-surface (Algorithm S2), unless  $p \in \{1, 2, \infty\}$ . This is discussed in the next section.

Algorithms V2 and S2 are not novel. They have already been presented in different formats in [4, 21]. In particular, [21] derives the density function of Algorithm S2 as well as its marginal distribution. Nevertheless, the distribution of Algorithm S2 is said to be “uniformly distributed on the surface of the (Lp-norm) unit sphere”, by definition or intuition, which is a claim contested here and discussed in the next section.

**Algorithms V2 and S2.** Simpler alternatives to Algorithms V1 and S1, respectively. Algorithm V2 is equivalent to Algorithm V1 for all  $p$ , while Algorithm S2 is equivalent to Algorithm S1 only for  $p \in \{1, 2, \infty\}$ . For other  $p$ , it fails to sample uniformly from the hyper-surface.

1. Sample  $Z_1, \dots, Z_n \sim \text{Gamma}(n/p)$ .
2. Let  $X_i \leftarrow Z_i^{1/p}$  for all  $i = 1, 2, \dots, n$ .
3. Let  $r \leftarrow \|(X_1, \dots, X_n)\|_p$  and  $\bar{X}_i \leftarrow X_i/r$  for all  $i = 1, 2, \dots, n$ .
4.  $\left\{ \begin{array}{ll} \text{For Algorithm V2 (volume),} & \text{sample } R \sim \text{Beta}(1, n). \\ \text{For Algorithm S2 (surface),} & \text{let } R \leftarrow 1. \end{array} \right.$
5. Sample signs  $S_1, \dots, S_n \sim \text{Uni}\{-1, 1\}$ .
6. Return  $(S_i \bar{X}_i R)_{i=1}^n$ .

The vector  $Z = (Z_1, Z_2, \dots, Z_n)$  in Algorithm V2 is  $p$ -isotropic. In particular, for  $p \in \{1, 2, \infty\}$ , this type of distribution is very used in physics, (mostly  $p \in \{2, \infty\}$  and  $n \in \{2, 3\}$ ), as well as in other areas of science and engineering. They are used, for instance, in the initialization and noise production for attacks to neural networks (mostly  $p = 2$ ,  $n \gg 1$ , e.g. Algorithm 1 in [19]), and in noise-injection for privacy applications including the laplace mechanism ( $p = 1$ ,  $n = 1$ ), metric-privacy ( $p = 1$ ,  $n \in \{2, 3\}$ ) [2] and differentially private stochastic gradient descent ( $p = 1$ ,  $n \gg 1$ ) in neural network training.

## 5.4 The Borel-Kolmogorov paradox

It is tempting to believe that Algorithm S2 generates samples that are uniformly distributed on the  $n$ -dimensional  $p$ -sphere, like Algorithm S1. After all, if the variable  $X$  is  $p$ -isotropic, its density can be written as a product

$$f_X(x) = f_{\bar{X}}\left(\frac{x}{\|x\|_p}\right) f_R(\|x\|_p), \text{ where } f_{\bar{X}}(\cdot) \text{ is a constant function.} \quad (10)$$

But such intuition contradicts the experiments in Figure 1 for  $p \notin \{1, 2, \infty\}$  as well as the main purpose of this paper.

This contradiction is a consequence of the Borel-Kolmogorov paradox. In the classic paradox, we consider a uniform distribution over a sphere and wish to express the conditional distribution restricted to a meridian line (half circumference) going from pole to pole.

By means of spherical coordinates, with a high resolution grid of latitudes and longitudes, one finds that if the domain is restricted to any thin lune bounded by consecutive longitudes, then the distribution of area is uniform over the lune while the distribution of latitudes is more concentrated around the equator, where the lune is thicker. As the resolution increases, the lune approaches a meridian path from pole to pole, and the distribution of latitudes converges to  $f_\theta(\theta) \propto \sin \theta$ , which is maximal at the equator ( $\theta = \pi/2$ ) and minimal at the poles ( $\theta \in \{0, \pi\}$ ).

But the distribution of longitudes for a fixed latitude does converge to a uniform distribution in  $[0, 2\pi]$ , which in turn implies a uniform distribution in  $[0, \pi]$  when the domain is restricted to one half of the equatorial circumference.

This difference between the distribution of latitudes on a fixed meridian line and that of longitudes over a half of the equatorial line contradicts conventional wisdom, because the two curves are identical and the spherical shape and the uniform distribution on its surface are invariant under rotations. There is no reason to believe that they should be different.

The solution to the paradox is that the conditional distribution given the a fixed event *depends* on the limiting procedure used to approach the event when the event has probability zero (a null event). This implies that conditional distributions on null events should always have a subscript indicating the limiting procedure, or a context from which it is obvious. According to [10], “...it is difficult to get people to see that the term ‘great circle’ is ambiguous until we specify what limiting operation is to produce it. The intuitive symmetry argument presupposes unconsciously the equatorial limit; yet one eating slices of an orange might presuppose the other.” He argued that in absence of information about a limiting procedure, it does not make sense to speak about conditional distributions given null events.

But recently, some researchers have proposed that in absence of a reference

limiting procedure the Hausdorff measure should be understood [3]. After all, the fact that there is no unique universal way of defining distribution on null events in a way that is invariant to the limiting procedure does not disprove that there is a default canonical limiting procedure. In this paper, we share and promote this view that the canonical  $k$ -dimensional measure in  $n$ -dimensions is the  $k$ -dimensional Hausdorff measure, defined and explained in full detail in [7]. Indeed, we have been referring to lengths of curves of surfaces in  $\mathbb{R}^n$  without questioning whether the curves have been approached as very thin worms or very thin rosaries or cones.

In the case of Algorithms S1 and S2, Equation (10) is indeed correct and the density  $f_{\bar{X}}$  is constant, but this does not imply that the distribution of  $\bar{X}$  is uniform over the  $p$ -sphere *in the canonical sense*. This is why the distribution generated by Algorithm S1 is uniform on the  $p$ -sphere (in the canonical sense), while that of Algorithm S2 is not. The latter ensures volumetric uniformity between two  $p$ -spheres of infinitesimally close  $p$ -radii, which is not the same as superficial uniformity unless  $p \in \{1, 2, \infty\}$ , as proven in Proposition 2.

## 6 Conclusion

This paper has shown that the  $p$ -norms  $p \in \{1, 2, \infty\}$  in  $n$ -dimensional space ( $n \geq 2$ ) are the only to enjoy of a volume-surface correspondence, meaning that when the volumetric uniform distribution inside the unitary  $p$ -ball ( $X \in \text{Ball}_p^n$ ) is projected to its surface ( $X/\|X\|_p \in \text{Sph}_p^n$ ) one obtains a uniform distribution on the surface.

Four algorithms for sampling uniformly from the volume and surface of the  $p$ -ball have been derived and they are implemented in Python in the Appendix. The first two are novel and based on squigonometry [24], while the last two are borrowed from the statistical works of [4, 21], two different perspectives that our paper aims to connect. The last two rely on the  $p$ -normal distributions, the only distributions to have a joint-isotropic property, meaning that the joint density of  $n$  i.i.d.  $p$ -normal random variables is radially symmetric in the  $p$ -norm.

Counterintuitively, the volume algorithms are equivalent in distribution, but the surface algorithms are not, unless  $p = \{1, 2, \infty\}$ . This is a crucial and unspotted observation in the literature whatsoever, and as we argue, it is tightly related to the Borel-Kolmogorov paradox produced by the parametrization with radius  $\|x\|_p$  and direction  $x/\|x\|_p$ .

## References

- [1] Luigi Amoroso. Ricerche intorno alla curva dei redditi. *Annali di matematica pura ed applicata*, 2:123–159, 1925.

- [2] Miguel E Andrés, Nicolás E Bordenabe, Konstantinos Chatzizokolakis, and Catuscia Palamidessi. Geo-indistinguishability: Differential privacy for location-based systems. In *Proceedings of the 2013 ACM SIGSAC conference on Computer & communications security*, pages 901–914, 2013.
- [3] Leon Bungert and Philipp Wacker. The lion in the attic—a resolution of the borel–kolmogorov paradox. *arXiv preprint arXiv:2009.04778*, 2020.
- [4] Stamatis Cambanis, Steel Huang, and Gordon Simons. On the theory of elliptically contoured distributions. *Journal of Multivariate Analysis*, 11(3):368–385, 1981.
- [5] Evan Chen. Monsters, an advanced handout which covers functional equations that have pathological solutions, 2016.
- [6] Keith Conrad. The gaussian integral. *University of Connecticut: Storrs, CT, USA*, pages 1–2, 2016.
- [7] Gerald A Edgar and Gerald A Edgar. *Measure, topology, and fractal geometry*, volume 2. Springer, 2008.
- [8] Edward Gaughan. *Introduction to analysis*, volume 1. American Mathematical Soc., exercise 4.39, 2009.
- [9] Irwin R Goodman and Samuel Kotz. Multivariate  $\theta$ -generalized normal distributions. *Journal of Multivariate Analysis*, 3(2):204–219, 1973.
- [10] Edwin T Jaynes. *Probability theory: The logic of science*. Cambridge university press, page 470, 2003.
- [11] Norman L. Johnson, Samuel Kotz, and Narayanaswamy Balakrishnan. *Continuous Univariate Distributions.*, volume 1. Wiley-Interscience, 1994.
- [12] Palaniappan Kannappan. *Functional equations and inequalities with applications*. Springer Science & Business Media, section 2.2, 2009.
- [13] Christian Kleiber and Samuel Kotz. *Statistical size distributions in economics and actuarial sciences*. John Wiley & Sons, 2003.
- [14] George Livadiotis. Expectation values and variance based on  $l_p$ -norms. *Entropy*, 14(12):2375–2396, 2012.
- [15] George Livadiotis. Chi- $p$  distribution: characterization of the goodness of the fitting using  $l_p$  norms. *Journal of Statistical Distributions and Applications*, 1:1–14, 2014.
- [16] Lillian MacArthur and Honglin Zhu. Classifying isometries. *arXiv preprint arXiv:2306.14909*, 2023.
- [17] Attila Gilányi (eds.) Marek Kuczma (auth.). *An Introduction to the Theory of Functional Equations and Inequalities: Cauchy’s Equation and Jensen’s Inequality*. Birkhäuser, 2 edition, 2009.

- [18] Khodabin Morteza and Alireza Ahmadabadi. Some properties of generalized gamma distribution. *Mathematical Sciences Quarterly Journal*, 4:11, 03 2010.
- [19] Marine Picot, Federica Granese, Guillaume Staerman, Marco Romanelli, Francisco Messina, Pablo Piantanida, and Pierre Colombo. A halfspace-mass depth-based method for adversarial attack detection. *Transactions on Machine Learning Research*, 2022.
- [20] Grant Sanderson. Why  $\pi$  is in the normal distribution (beyond integral tricks). Youtube animation, 2023.
- [21] Danhong Song and A Gupta. Lp-norm uniform distribution. *Proceedings of the American Mathematical Society*, 125(2):595–601, 1997.
- [22] Edney W Stacy. A generalization of the gamma distribution. *The Annals of mathematical statistics*, pages 1187–1192, 1962.
- [23] E Hewitt-K Stromberg et al. Real and abstract analysis. *Graduate Texts in Math*, 18, exercise 18.46, 1965.
- [24] William E Wood and Robert D Poodiack. Squigonometry: Trigonometry in the p-norm. *A Project-Based Guide to Undergraduate Research in Mathematics: Starting and Sustaining Accessible Undergraduate Research*, chapters 3 and 7, 2020.

## A Appendix

### Python implementation of the algorithms

For Algorithms [V2](#) and [S2](#), sampling from  $f_p$  can be done using a generalized gamma distribution.

For Algorithms [V1](#) and [S1](#), there are more difficulties. In order to sample  $T_k$  from  $f_{T_k}$ , one can use an approximation by literally creating a grid with a large number of points that discretizes the unsigned  $p$ -circumference in 2D, spaced conveniently to improve precision at the critical points  $t = 0$ ,  $t = \pi/4$  and  $t = \pi/2$ . This produces cumulative density functions whose inverse can then interpolate at random values in  $(0, 1)$ .

```
import numpy as np
from scipy.stats import gengamma
from functools import lru_cache # Python's standard library

def sample_generators(p: float, n: int, q=None, grid_precision: int = 100000):
    if q is None:
        q = p
```



```

def gen_volume(N):
    if p == np.inf:
        x = np.random.random(size=(N, n))
    else:
        x = gengamma(a=1 / p, c=p).rvs(size=(N, n))
    r = np.linalg.norm(x, ord=p, axis=-1, keepdims=True)
    u = np.random.random(size=(N, 1))
    x = x * np.random.choice([-1, 1], size=x.shape)
    return x / r * u ** (1 / n)

def gen_surface(N):
    if p in (1, 2, np.inf): # Use volume projection (faster)
        x = gen_volume(N)
        return x / np.linalg.norm(x, ord=p, axis=-1, keepdims=True)

    x = np.empty((N, n))
    x[:, 0] = 1
    x_grid, y_grid = grid_info["x"], grid_info["y"]
    for k in range(2, n + 1):
        u = np.random.random(N)
        x_k = np.interp(u, xp=t_k_curve(k), fp=x_grid)
        y_k = np.interp(u, xp=t_k_curve(k), fp=y_grid)
        x[:, k - 1] = x_k
        x[:, : k - 1] *= y_k[:, None]
    x *= np.random.choice([-1, 1], size=x.shape)
    return x

# Auxiliary functions for surface sampling

@lru_cache(maxsize=n) # cache to avoid recomputations
def t_k_curve(k):
    y, dLq = grid_info["y"], grid_info["dLq"]
    cum_t_k = np.cumsum(y ** (k - 2) * dLq)
    return cum_t_k / cum_t_k[-1]

def p_circumference_grid():
    # (x,y) are the points in the p-circumference. w is y^p.
    # w_eps = min(0.05, max(1 / grid_precision ** (q * p), 1e-16))
    geom = np.geomspace(1e-16, 0.1, num=int(0.05 * grid_precision))
    lin = np.linspace(0.1, 0.4, num=int(0.4 * grid_precision))
    w = np.array([0, *geom, *lin, *(0.5 - geom[::-1])])
    w = np.unique(np.sort([0, *w, 0.5, *(1 - w[::-1]), 1]))
    y = w ** (1 / p) if p < np.inf else np.minimum(2 * w, 1.0)
    x = (1 - w) ** (1 / p) if p < np.inf else np.minimum(2 * (1 - w), 1.0)
    dY = np.diff(y, prepend=0)
    dX = np.diff(x, prepend=1)

```

```

dA = (0.5 * dX * y + 0.5 * x * dY) - y * dX
t = 2 * np.cumsum(dA)
dLq = np.linalg.norm([np.abs(dX), np.abs(dY)], ord=q, axis=0)
Lq = np.cumsum(dLq)
pi_p, piL_pq = t[-1] * 2, Lq[-1] * 2
return dict(t=t, x=x, y=y, Lq=Lq, dLq=dLq), pi_p, piL_pq

grid_info, pi_p, piL_pq = p_circumference_grid()

return gen_volume, gen_surface, pi_p, piL_pq

# Usage example
gen_volume, gen_surface, *_ = sample_generators(p=1.5, n=3)
xyz_v = gen_volume(10000)
xyz_s = gen_surface(10000)

# Plot
import plotly.graph_objects as go
_kw = dict(mode="markers", marker=dict(size=2))
kw = lambda xyz: dict(x=xyz[:, 0], y=xyz[:, 1], z=xyz[:, 2], **_kw)
fig = go.Figure()
fig.add_trace(go.Scatter3d(**kw(xyz_v)))
fig.add_trace(go.Scatter3d(**kw(np.abs(xyz_s))))
fig.show()

```

